23rd ABCM International Congress of Mechanical Engineering
December 6-11, 2015, Rio de Janeiro, RJ, Brazil

AEROELASTIC FLUTTER OPTIMIZATION THROUGH FIBER ORIENTATION

Guilherme Roldo
Jun S. O. Fonseca
Universidade Federal do Rio Grande do Sul, Porto Alegre, Rio Grande do Sul, Brasil
guilhermeroldo@gmail.com, jun@ufrgs.br
Carlos E. de Souza
Universidade Federal de Santa Maria, Santa Maria, Rio Grande do Sul, Brasil
carlos.souza@ufsm.br

Abstract. *This paper discusses an aeroelastic tailoring methodology that aims the increase of flutter onset speed of flat plates using the ply orientation as design variable. The search for a very light aircraft design and the design of small unmanned aerial vehicles (UAVs) lead to the use of laminate composite material and only a few layers of material. Each ply is usually a commercial unidirectional tape or bi-directional plain weave fabric with specified thickness. Many times, the designer is left then with the choice of each ply orientation definition for aeroelastic requirements, such as flutter speed increase. The flutter solution is obtained here from a stability analysis of the aeroelastic equation of motion in its generalized form, through ZONA6 panel method for subsonic flow from commercial software ZAERO. The structural normal modes and frequencies are obtained via finite element method using an 8-node degenerated shell element code. The flutter onset speed is maximized by unconstrained sequential linear programming with fiber orientation as design variables. The sensitivity to the fiber orientation at each ply is approximated by forward finite difference. Flat plates with one and two ply orientations are studied in this work. The proposed procedure was able to increase flutter speed up to a factor of three, though, for some cases, the optimized fiber orientations found provides less than the possibly achievable flutter speed when the algorithm encounters a local maximum. A few number of optimization runs with starting orientations set at random could help finding the global maximum.*

Keywords: *aeroelastic tailoring, flutter optimization, fiber orientation*

1. INTRODUCTION

Unmanned aerial vehicles (UAVs) capable of soaring at high altitudes, for long periods of time and with low fuel consumption have to be designed in order to maximize the produced lift, minimize weight and reduce drag as much as possible. For such vehicles, a wing form with long span – so the planform area is increased, thus increasing lift – and high aspect ratio – as it reduces drag induced by wingtip vortices – are desirable. The combination of high stiffness and strength-to-weight ratio of composite materials also make their use advantageous for efficient UAV design. Nonetheless, the long span and reduced wing cross area associated with lower mass and stiffness of composite materials – compared to those of traditional materials – are likely to present high displacements and vibrational issues. Aeroelastic flutter is a potentially destructive and unstable phenomenon that happens when one or more vibrational modes of the structure couple with aerodynamic forces.

UAV's have been initially developed for military operations, such as enemy territory reconnaissance, and are now finding a niche on civilian applications, making customary tasks – aerial inspection of crops and electric lines, car traffic observation, environmental monitoring, among others – easier, remotely controlled and possibly cheaper.

Aeroelastic tailoring was defined by Shirk and Weisshaar (1986) as " the embodiment of directional stiffness into an aircraft structural design to control aeroelastic deformation, static or dynamic, in such a fashion as to affect the aerodynamic and structural performance of that aircraft in a beneficial way". Fiber-reinforced laminae present orthotropic mechanical properties, which can be manipulated by changing fiber orientation on the lamina. A structure is usually composed of at least a few laminae, so fibers at each lamina can be placed in the most convenient orientation, according to the designer's purpose.

A more extensive review of previous works on the subject of aeroelastic tailoring was put together by Jutte and Stanford (2014). Several different strategies have been used for aeroelastic tailoring, including fiber tow steered composites, functionally graded materials, selectively reinforced material, smart materials, non-conventional structural design, among others.

In this work, finite element method is used to obtain mass and stiffness matrices for the structure which are used to solve the modal eigenproblem for natural frequencies and vibrational modes. These are fed into ZAERO, a widely used commercial software which performs unsteady aerodynamics calculations to estimate flutter onset speed. The ply orientation that maximizes the flutter speed is found through sequential linear programming (SLP). Objective function is evaluated at each optimization step and its sensitivity to design variables is evaluated by forward finite difference.

2. AEROELASTICITY

Aeroelasticity is the field of studies interested in phenomena occurring when excitations of three different kinds – aerodynamics excitations, structural elastic and structural vibrations – interact with each other, creating a combined system's response.

Aeroelastic flutter is a dynamically instability that occurs when one or more of the structure's vibration modes couples with aerodynamic forces, at this point, the structure no longer damps the vibrations and the energy associated with the phenomenon goes up, increasing its amplitudes. Flutter can cause a series of undesirable effects, such as, inefficient flight, loss of aircraft control, and damage to secondary or primary structures. Flutter starts when airflow speed equals the flutter onset speed of the structure. Understandably , aircraft design should guarantee flutter occurrence to be outside of the aircraft flight envelope.

Traditionally, during aircraft design aeroelastic effects are only taken into account at final stages of design process. However, modern day design practice has been more attentive in respect to aeroelastic design, and more effort is being employed on earlier stages of the design process to prevent such phenomena.

The equation of motion for the aeroelastic undamped system with its associated forces can be written as in Eq. 1. $\mathbf{M}$ and $\mathbf{K}$ are the mass and stiffness matrices for the discretized system, $\mathbf{x}$ is the structural deformation vector and $\mathbf{F}$ is the force vector.

$$\mathbf{M}\ddot{\mathbf{x}}(t) + \mathbf{K}\mathbf{x}(t) = \mathbf{F}(t) \tag{1}$$

The forces represented by the $\mathbf{F}$ vector can be distinguished into two different groups, accordingly to its source: external forces $\mathbf{F_e}(\mathbf{t})$ and deformation-dependent forces $\mathbf{F_a}(\mathbf{t})$. The former encompasses forces like wind gusts, atmospheric turbulence and forces induced by pilot input for control surfaces movements. The latter are forces that are modifies according to the structural deformation of the structure. As $\mathbf{F_a}(\mathbf{t})$ is dependent on structural deformations, this can be regarded as an aerodynamics feedback on the aeroelastic system, as depicted in Fig. 1

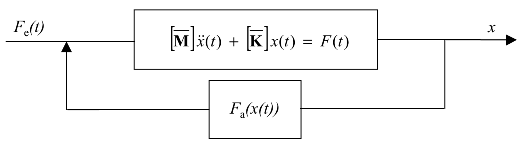

Figure 1: Box representation of aerodynamic feedback on aeroelastic systems.

Usual practice in flutter analysis is to recast the problem into the Laplace domain as a set of linear systems, which requires the assumption of amplitude linearization – the aerodynamic response is linear with respect to the amplitude of structural deformation if the amplitude is sufficiently small. The size of the problem is also reduced by solving it in the generalized space, where the generalized mass and stiffness matrices, $\bar{\mathbf{M}}$ and $\bar{\mathbf{K}}$, are expressed as in Eq. 2 and Eq. 3.

$$\bar{\mathbf{M}} = \mathbf{\Phi^T M \Phi} \tag{2}$$

$$\bar{\mathbf{K}} = \mathbf{\Phi^T K \Phi} \tag{3}$$

This simplifications allows Eq. 1 to be rewritten as:

$$\left[s^2\bar{\mathbf{M}} + \bar{\mathbf{K}} - q_\infty \mathbf{Q}\left(\frac{sL}{V}\right)\right]\mathbf{q} = 0, \tag{4}$$

Equation 4 is known as the classical flutter matrix equation, where $\bar{\mathbf{M}}$ and $\bar{\mathbf{K}}$ are the mass and stiffness matrices in the generalized space. To perform the aeroelastic calculations ZAERO's ZONA6 method is employed in this work. A wider and detailed discussion on flutter prediction and the solution of the aeroelastic problem can be found in ZONA (2011).

2.1 STRUCTURAL PROBLEM

In this work, finite element method is employed for the structural analysis. A shell element derived from the degeneration of a solid element is applied, as proposed by Ahmad *et al.* (1970). A review of this element can be found in Zienkiewicz and Taylor (2000).

First-order Shear Deformation Theory (FSDT) allows the calculation of the constitutive matrix for laminated materials. In FSDT, Kirchhoff hypothesis is relaxed so that straight lines normal to the mid-surface before deformation do not necessarily remain normal to the mid-surface after deformation. This allows for the introduction of shear strain in the theory. In comparison to classical lamination theory, FSDT provides better relation between computational efficiency and accuracy Zhang and Yang (2009).

The stiffness matrix is assembled following the formulation presented by Kumar and Palaninathan (1997), where the transverse integration on the element is accomplished assuming constant inverse isoparametric mapping Jacobian matrix, and the computations are carried out only on the reference surface:

$$\mathbf{K_e} = \int_{-1}^{1}\int_{-1}^{1} \left(\mathbf{B_1^T C_1 A B_1} + \mathbf{B_1^T C_2 B_2} + \mathbf{B_2^T C_2 B_1} + \mathbf{B_2^T C_3 B_2}\right) \frac{2}{t}|\mathbf{J}| d\xi_1 d\xi_2, \tag{5}$$

where $\mathbf{B}$ is the coordinate transformation matrix:

$$\mathbf{B} = \mathbf{B}_1 + z\mathbf{B}_2. \tag{6}$$

where matrices $\mathbf{B}_1$ and $\mathbf{B}_2$ are the strain-displacement matrices, t is the total element thickness and $\mathbf{J}$ is the Jacobian. The constitutive tensors above are defined here as:

$$\mathbf{C}_1 = \sum_{k=1}^{nl} \overline{\mathbf{C}}_k (z_t - z_b)_k\ , \quad \mathbf{C}_2 = \sum_{k=1}^{nl} \overline{\mathbf{C}}_k (z_t^2 - z_b^2)_k\ , \quad \mathbf{C}_3 = \sum_{k=1}^{nl} \overline{\mathbf{C}}_k (z_t^3 - z_b^3)_k\ . \tag{7}$$

In these equations, n_l is the element number of plies and z_t and z_b are the ply top and bottom coordinates. The stiffness matrix $\overline{\mathbf{C}}_k$ is function of the ply orientation, and is obtained trough a plane rotation of $\mathbf{C}_k$, which is expressed in the layer coordinate system:

$$\overline{\mathbf{C}_k} = \mathbf{T}_{pl}^T(\theta)\mathbf{C}_k\mathbf{T}_{pl}(\theta) \tag{8}$$

When considering only plane stress state, $\mathbf{C}_k$ is a plane-stress reduced stiffness matrix with elements given by equations (4.4-3b) e (4.4-3c) of Ref. Reddy (2004):

$$\mathbf{C} = \begin{bmatrix} C_{11} & C_{12} & 0 & 0 & 0 \\ C_{12} & C_{22} & 0 & 0 & 0 \\ 0 & 0 & C_{44} & 0 & 0 \\ 0 & 0 & 0 & C_{55} & 0 \\ 0 & 0 & 0 & 0 & C_{66} \end{bmatrix}, \quad \begin{array}{l} C_{11} = E_1/(1-\nu_{12}\nu_{21}) \\ C_{22} = E_2/(1-\nu_{12}\nu_{21}) \\ C_{12} = \nu_{12}E_2/(1-\nu_{12}\nu_{21}) \\ C_{44} = G_{23} \\ C_{55} = G_{13} \\ C_{66} = G_{12} \end{array} . \tag{9}$$

The plane rotation matrix $\mathbf{T}_{pl}$ is given by:

$$\mathbf{T}_{pl}(\theta) = \begin{bmatrix} c^2 & s^2 & 0 & 0 & cs \\ s^2 & c^2 & 0 & 0 & -cs \\ 0 & 0 & c & -s & 0 \\ 0 & 0 & s & c & 0 \\ -2cs & 2cs & 0 & 0 & c^2 - s^2 \end{bmatrix} \text{where} \quad c = \cos(\theta) \text{ and } \ s = \sin(\theta). \tag{10}$$

Further discussion on composite materials and the formulation for FSDT can be found on composite books, such as Reddy (2004) and Jones (1999).

2.1.1 Modal Eigenproblem

The dynamic behavior of a structure can be characterized by natural frequencies and vibrational modes. Assuming the structure motion as harmonic oscillation, nodal displacement is written as a sinusoidal function. Displacement acceleration vectors can be expressed as in Eq. 11 and Eq. 12:

$$\mathbf{x} = \sin(\omega t), \tag{11}$$

$$\ddot{\mathbf{x}} = \frac{\partial^2 \mathbf{x}}{\partial t^2} = -\omega^2 \sin(\omega t). \tag{12}$$

The equation of motion for the undamped and free oscillating system are expressed as in Eq. 13:

$$\left(\mathbf{K} - \omega_i^2 \mathbf{M}\right) \mathbf{\Phi}_i = 0. \tag{13}$$

The eigenproblem in Eq. 13 can be solved for the eigenvalues ω_i, which are the structure's natural frequencies, and the eigenvectors $\mathbf{\Phi_i}$, which are its corresponding vibrational modes.

3. OPTIMIZATION

Optimization problems are a set of problems that seek to find the values of independent variables that when substituted into a specific function minimizes (or maximizes) the value of that function. It can be chosen to solve the problem so that desired inequalities are to be satisfied, limiting the range of possible independent variables. Equation 14 shows a general constrained optimization problem.

$$\begin{aligned} &\min_x f(x) \\ &\text{subject to x} \leq 0 \end{aligned} \tag{14}$$

In the scope of this work, the optimization problem is to maximize the flutter onset speed $V_f(\theta)$, so that flutter is pushed out of the flight envelope boundaries. The optimization of flutter speed must be achieved by finding the optimum ply stacking sequence, θ. Here, the optimization problem is unconstrained and design variables are continuous can assume any value in the range $-90° \leq \theta \leq 90°$. The general optimization problem can be rewritten to this particular case as in Eq. 15.

$$\max_\theta V_f(\theta) \tag{15}$$

Recent work by Varella *et al.* (2012) have proposed that both flutter speed and its associated natural frequency have a similar behavior with respect to fiber orientation, so that minima and maxima for both functions happened for the same values of θ. In this work, the number of flutter speed calculations is reduced to only two evaluations throughout the optimization process. The first assessment of V_f was calculated for the provided initial guess of θ and the second was calculated after θ had converged to verify the flutter speed increased. The computer-cost saved by reducing the number of objective function evaluations makes the code very fast. The natural frequency of the flutter mode was maximized, in order to improve the aeroelastic response of the structure.

DeLeon *et al.* (2012) uses a more sophisticated approach, in which finite difference is used to evaluate the sensitivity of V_f in relation to each eigenvalue. The most signifcant eigenvalue is then maximized by finding the optimum θ.

In the present work, at each optimization step flutter speed is reevaluated and its sensitivity in relation to each design variable is obtained. Linear programming is then used to update the values of the design variables. It is not trivial to establish an analytical expression to relate the dependency of the flutter speed to the fiber orientation. Thus, the sensitivity analysis is performed through the forward finite difference method, where a small perturbation $\Delta\theta_i$ is applied to the design variable and the objective function is reevaluated at this point and the derivative of the objective function can be approximated. Equation 16 depicts the sensitivity approximation though finite difference method, where i is the ply index.

$$\frac{\partial V_f(\theta)}{\partial \theta_i} = \frac{V_f(\theta + \Delta\theta_i) - V_f(\theta)}{\Delta\theta_i} \tag{16}$$

With such formulation, the methodology differs from DeLeon *et al.* (2012) and Varella *et al.* (2012), as the problem becomes not to maximize the natural frequency and expect a indirect result on flutter speed. Instead, the proposed methodology assures flutter speed is being maximized at each step.

4. NUMERICAL STUDIES

A low aspect ratio flat plate made of composite laminae, subjected to airflow is the study object of this work. Specimens geometrical configuration and loading are shown in Fig. 3. Each plate is composed of one or two plies, having a total thickness of $15mm$. The material used is epoxy matrix with carbon fiber reinforcement. Properties for this material are presented in Fig. 3, as obtained in Lebkuchen *et al.* (2013). Index 1 and 2 correspond to properties in parallel and perpendicular to fiber direction, respectively.

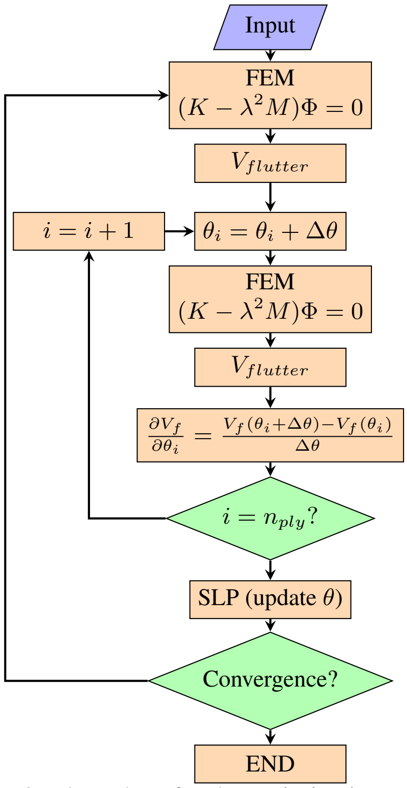

Figure 2: Flow chart for the optimization process.

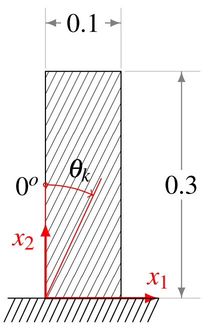

$E_1[GPa]$	92.7
$E_2[GPa]$	6.7
$G_12[GPa]$	4.35
ν	0.25
$\rho[kg/m^3]$	1427

Figure 3: Laminated plate model with material properties (experimental results for flexural properties of CFRC-4HS and CFRC-TWILL composites. Span/depth ratio = 35:1. Average results of 7 specimens.)

4.1 Modal Analysis Validation

To validate the formulation of the finite element method, experimental data was used. Experimental modal analysis(EMA) results found in Lebkuchen *et al.* (2013) were compared to numerical calculations from two FEM softwares: ABAQUS and CSOpt. The experimental work assesses the modal behavior of five plates with geometry as in Fig. 3. Each plate has a single ply orientation, with θ varying from 0° to 90°. Table 1 shows the frequencies found in Lebkuchen *et al.* (2013) for the 1^{st} and 2^{nd} bending modes as well as the 1^{st} torsion mode and compares them with numerical results.

Figure 4a show the evolution of the plate dynamic behavior changes with increasing theta, comparing experimental and numerical results. Figure 4b compares the results from ABAQUS and CSOpt only, as no experimental data was available.

In Fig. 4a, experimental points are compared to frequency curves obtained with ABAQUS and CSOpt. Numerical methods can be seen to slightly overestimate the structure's natural frequencies due to simplified assumptions about the strucure's boundary conditions. Though, this overestimation is under 0.5 for all cases. In Fig. 4a and Fig. 4b, both numerical methods have strongly agreed in their results. This proves the efficiency of the home-built code CSOpt in dealing with this set of modal problems.

Table 1: Dynamic behavior of single ply plate with increasing θ. Experimental and numerical results are compared.

θ_k	Frequencies (Hz)								
	1^{st} bending			1^{st} torsion			2^{nd} bending		
(°)	EMA	ABAQUS	CSOpt	EMA	ABAQUS	CSOpt	EMA	ABAQUS	CSOpt
0.0	20.8	21.72	21.70	130.37	136.35	135.45	53.12	56.53	55.43
30.0	9.7	11.11	11.12	59.12	60.87	60.16	84.75	88.73	87.91
45.0	7.2	8.08	8.10	44.12	49.10	48.79	67.12	70.87	70.04
60.0	6.6	6.60	6.61	39.50	41.09	40.86	57.25	57.36	56.51
90.0	5.7	5.83	5.83	35.25	36.67	36.43	45.87	46.51	45.57

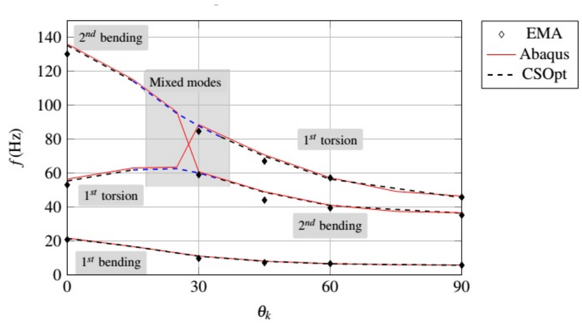

(a) Dynamic behavior of single ply plate with increasing θ. Experimental and numerical results are compared.

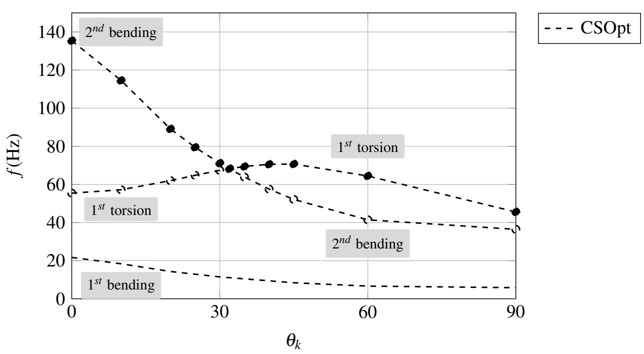

(b) Numerically assessed dynamic behavior of two plies plate with increasing θ.

4.2 Optimization Results

Flutter behavior of plates with one and two plies is obtained so that flutter onset speed relation to fiber orientation is known in advance. Flutter onset speed is evaluated for θ in the range of 0 to 90° and increments of 5°. Knowing the behavior of flutter, V_f, as a function of θ beforehand serves only as a benchmark to understand the optimizer processing. This stage is not necessary during optimization.

Next, a stack sequence is stochastically chosen for the initial values of θ and undergoes the optimization process. This procedure is repeated a few times.

4.3 Single Ply Plate

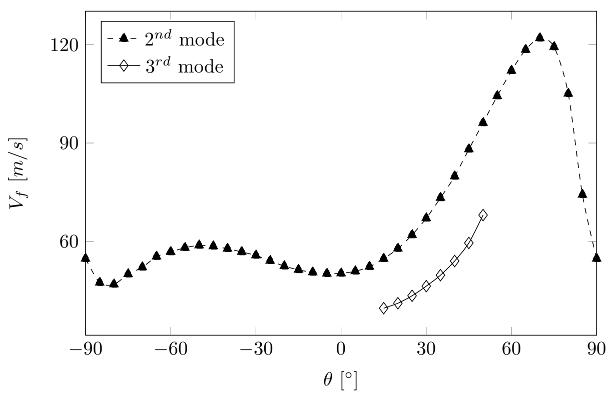

(a) Flutter speed of single ply plate as function of θ.

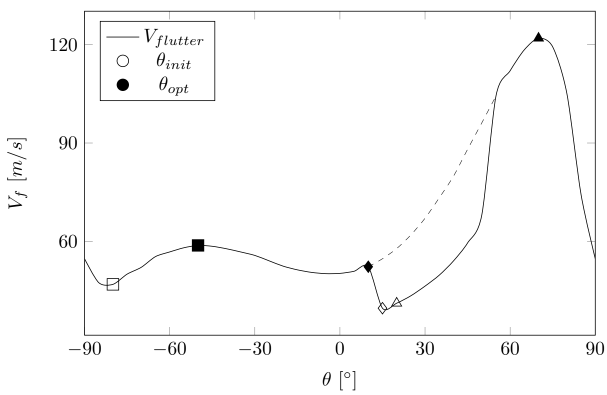

(b) Results for aeroelastic optimization of single ply plate.

Figure 5: Results for a single ply plate.

Figure 5a depicts the fiber orientation effects on flutter behavior for a single ply plate. First point to observe is that contrary to natural frequency, flutter speed is not symmetrical in relation to $\theta = 0°$. This opposes the assumptions made by DeLeon *et al.* (2012) and Varella *et al.* (2012) that optimization of natural frequency is sufficient to assure the optimization of flutter speed. Although frequencies are symmetrical about $\theta = 0°$, vibration modes mirrored about that axis. Flutter is dependent on natural frequencies, but also depends on aerodynamics load distribution, being so, a mirrored modal shape in relation to the airflow can greatly interfere with aeroelastic behavior.

Second and third modes are the associated flutter modes. In the region $15° \leq \theta \leq 50°$ both modes are present, although, in practice, only the third mode would cause flutter, as it appears at much lower speeds. Third mode appearance causes a discontinuity on the flutter speed behavior, which could be troublesome for the optimizer. This region is more or less coincident to the region of mixed modes in Fig. 4a, indicating that modes which are torsion-bending coupled modes could be more prone to low flutter speeds. Third mode holds both maxima, at θ around -50 and 70 degrees.

Figure 5b shows initial values for θ and the optimization results. For all runs the optimizer was able to find the local maxima, what is expected of a gradient based optimizer. The three maximum are the the points: $(-48°, 58\ m/s)$, $(15°, 53\ m/s)$ and $(72°, 122\ m/s)$. Both local maxima present V_f values much lower than the global maximum. In fact, the values are less than half of that for global maximum. Also, when the optimizer reaches the maximum $(15°, 53\ m/s)$, it does not perceive 2^{nd} mode associated speeds keep rising, and it stops at that point, to avoid falling into the 3^{rd} mode much lower speeds.

4.4 Two Plies Plate

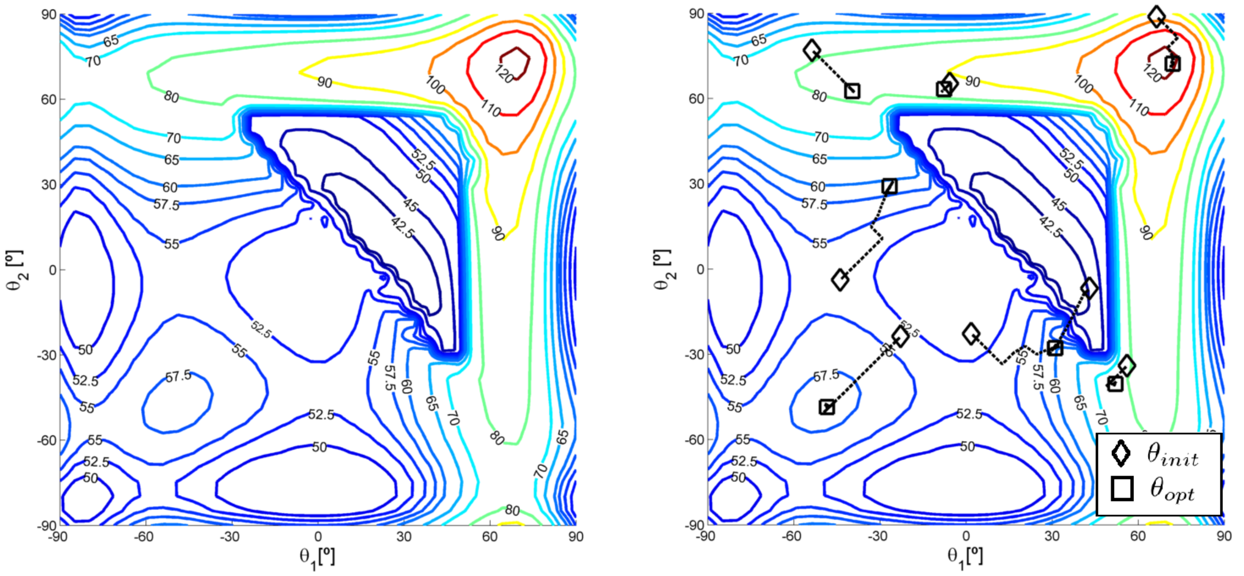

(a) Flutter speed as a function of θ_1 and θ_2. (b) Optimization path for 11 random initial orientations. 1

Figure 6: Results for a plate with two plies.

Figure 6a presents the flutter speed behavior of a plate with two plies, horizontal and vertical axis are the values of fiber orientation, whereas contour lines show the flutter onset speed for each combination of θ_1 and θ_2 values. V_f is almost symmetric in relation to the $\theta_1 = \theta_2$ diagonal, which is the domain studied in 4.3. Global maximum occurs at the same point as in 4.3, as well as the local minimum.

Figure 6b shows how the path taken between each initial choice (marked with diamonds) of θs and the found optimum (marked with squares). Once again, the algorithm has proven its efficiency in increasing V_f and its limitations were the convergence to local maxima, which leads to much lower values of V_f than the possible achievable.

5. CONCLUSION

The proposed optimization procedure proposed in this work has evidenced its ability to be employed on aircraft design when flutter speed is demonstrated to be an issue. The use of different ply stacking configurations, taking advantage of the directional properties of composite materials, has shown to be an excellent artifice for tailoring the structure's stiffness without adding weight penalties or changing geometry.

The results achieved on each optimization run were heavily dependent on the choice of initial stacking sequence, a poor starting configuration could take the algorithm to converge to e a local maximum. In the studied cases local maxima presented much worst flutter performance compared to the global maximum. The choice of a good starting stacking sequence relies on deep understanding of the phenomena and possibly on a few flutter calculations beforehand. This issue could possibly be overcome by running the optimization for a few initial configurations, picked at random or based on prior knowledge, when some information on structure's flutter behavior is available. Then, the best results among these universe could be picked as maximum. This trick could become prohibitive when the evaluation of flutter onset speed have a high computational cost and time consumption for unsteady aerodynamics calculation is bigger than time spent in solution of linear programming.

Although the simple models studied in this work were not enough to represent a real wing at full, it was sufficient to demonstrate the influence of stacking sequencing on aeroelastic performance and the potential on paying extra attention to the choice of orientations not only during stiffness and displacement analysis.

The procedure and results presented in this work contributes to the vast range of tools available for aeroelastic tailoring, facilitating the design of more efficient, lighter and faster aircrafts.

6. ACKNOWLEDGMENTS

To CNPq (Conselho Nacional de Desenvolvimento Científico e Tecnológico) for the financial support to G. Roldo and J. S. O. Fonseca.

7. REFERENCES

Ahmad, S., Irons, B. and Zienkiewicz, O., 1970. "Analysis of thick and thin shell structure by curved finite elements". *International Journal for Numerical Methods in Engineering*.

DeLeon, D., de Souza, C., Fonseca, J. and da Silva, R., 2012. "Aeroelastic tailoring using fiber orientation and topology optimization". *Structural and Multidisciplinary Optimization*, pp. 663–677.

Jones, R., 1999. *Mechanics of Composite Materials*. Scripta Book Company, Washington, 2nd edition.

Jutte, C. and Stanford, B., 2014. "Aeroelastic tailoring of transport aircraft wings: State-of-the-art and potential enabling technologies". *NASA Technical Memorandum*.

Kumar, W. and Palaninathan, R., 1997. "Finite element analysis of laminated shells with exact through-thickness integration". *Computer and Structures*, , No. 63(1), pp. 173–184.

Lebkuchen, H., Marto, A. and de Souza, C., 2013. "Modal parameters fitting of composite flat plates for aeroelastic analysis". *22nd International Congress of Mechanical Engineering*.

Reddy, J., 2004. *Mechanics of Composite Plates and Shells - Theory and Analysis*. 2nd edition.

Shirk, M., H.T. and Weisshaar, T., 1986. "Aeroela stic tailoring Ű theory, practice, promise,". *Journal of Aircraft*, Vol. 23, No. 1, pp. 6–18.

Varella, G., De Leon, D., Fonseca, J., de Souza, C. and da Silva, R., 2012. "Orientaion optimization for the flutter onset in reinforced laminated plates using mac". *Computational Mechanics Proceedings*.

Zhang, Y. and Yang, Z., 2009. "Recent developments in finite element method analysis for laminated composite plates". *Composite Structures 88*, pp. 147–157.

Zienkiewicz, O. and Taylor, R., 2000. *The Finite Element Method - The Basis*, Vol. volume 1. Elsevier Academic Press, 5th edition.

ZONA, T.I., 2011. *ZAERO Theoretical Manual*. ZONA Technology Inc., Scottsdale, Arizona, USA, 21st edition.

8. RESPONSIBILITY NOTICE

The authors are the only responsible for the printed material included in this paper.